

## TEST AND ANALYSIS OF RC CURVE BEAMS UNDER REVERSED CYCLIC IN-PLANE LOADS

Maw-Shyong SHEU<sup>1</sup>, Yih-Houng CHEN<sup>2</sup> And Chi-Huang CHEN<sup>3</sup>

### SUMMARY

Fifteen full scale RC curve beams are tested under two concentrated in-plane loads with one or multiple reversed cycles. The cross-section of curve beam is 25cm × 40cm with 110cm interior radius and 150cm exterior radius.  $f'_c$  changes from 22.4 to 34.4 Mpa;  $f_y$  of rebar is from 384.7 to 533.5 Mpa;  $f_y$  of stirrup and hanger is from 397.8 to 508.4 Mpa.  $\rho$  and  $\rho'$  vary from  $14/f_y$  to  $\rho_b$ . All the specimens fail in flexure or shear. After test, the flexural cracking load, flexural ultimate load, shear cracking load, shear ultimate load and effective cross-sectional area are calculated. In order to simplify the design process, equivalent rectangular stress block for ultimate bending capacity is also introduced in this paper. The analytical load-deflection curve under monotonic load is predicted and compared to the experimental result with reasonable accuracy.

### INTRODUCTION

Arch roofs, arch bridges, tunnels and sewage ducts are very popular curve structures. However, most of the RC design codes do not specify clearly the design equations for curve structures. Curve beams can not be designed using equations for straight beams. Because the tangential strain across the curve beam cross-section is hypobolic instead of straight distribution when subjected to bending moment[1]. The purpose of this paper is to investigate the flexural capacity, shear capacity and effective stiffness of RC curve beams under in-plane static loads. Finally, the equivalent stress block of RC curve beams at ultimate flexural state is also proposed.

### EXPERIMENTAL TEST

Table 1 is the parameters of the specimens. The cross-section of all specimens is 25cm × 40cm with interior radius 110cm and exterior radius 150cm.  $\rho$  and  $\rho'$  are from  $14/f_y$  to  $\rho_b$  for straight beam. Two concentrated in-plane loads are applied at one-third points under one or multiple reversed cycles. Fig.1 shows the experimental set up where two rollers are inserted at both supports. In general, member ductility would be larger than 2.5, if  $\rho \leq 0.5\rho_b$  and  $\rho' > 0.5\rho$  for flexural curve beams as shown in Fig.2. Fig.3 and Fig.4 are the crack patterns at final states for flexural failure and shear failure.

### ANALYTICAL STRENGTH OF CURVE BEAMS

Consider a segment of curve beam subjected to bending moment as shown in Fig.5. The radii of curvature of neutral axis before and after bending are  $r_{na}$  and  $r'_{na}$ . Let  $r$  be the radius of curvature of any tangential fiber before bending. The tangential elongation of that fiber is  $(r_{na} - r)(d\phi - d\phi')$ . So the tangential compression strain of this fiber becomes :

$$\varepsilon = (r_{na} - r)(d\phi - d\phi') / (rd\phi)$$

<sup>1</sup> Department of Architecture, National Cheng-Kung University, Tainan, Taiwan. Email: mssheu@mail.ncku.edu.tw

<sup>2</sup> Department of Architecture, National Cheng-Kung University, Tainan, Taiwan

<sup>3</sup> Department of Architecture, National Cheng-Kung University, Tainan, Taiwan

or

$$\varepsilon = \frac{(r_{na} - r)}{r} \left( 1 - \frac{r_{na}}{r'_{na}} \right) \quad (1)$$

where  $r_{na}$  and  $r'_{na}$  are unknowns. However, for a prescribed strain  $\varepsilon_p$  at a given fiber  $r_p$ , Eq.(1) may be expressed as function of that prescribed condition :

$$\varepsilon = \frac{(r_{na} - r)}{r} \left( \frac{\varepsilon_p r_p}{r_p - r'_{na}} \right) \quad (2)$$

For instance if  $r_p = r_i$ ,  $\varepsilon_p = +0.623\sqrt{f'_c}/E_c$ , Eq.(2) gives the hypobolic strain distribution at the cross-section where positive cracking moment occurs. If  $r_p = r_o$ ,  $\varepsilon_p = 0.003 + 0.02b/z + 0.2\rho_s$ , Eq.(2) gives the strain distribution at the cross-section where positive ultimate moment occurs. By try and error process, the location of neutral axis,  $r_{na}$ , may be found for equilibrium. Using Eq.(2), the tangential strain and stress of concrete and rebars at a cross-section can be calculated for any prescribed condition. Comparing the analytical solutions with experimental results, the error for the load of cracking moment is -20% to +18%; the error for the load of ultimate moment is -14% to +17%.

The ultimate shear capacity of curve beam,  $V_u$ , is similar to the ultimate shear capacity of straight beam. In other words,  $V_u$  is contributed by concrete  $V_c$ , stirrup  $V_s$ , dowel force of tensile rebars  $V_d$ , and component of tensile force of rebars.  $V_c$  is proposed by this paper as :

For axial compression

$$V_c = 0.175 \left( 1 + \frac{N}{14A_g} \right) \sqrt{f'_c} bd \quad (3)$$

For axial tension

$$V_c = 0.175 \left( 1 - \frac{N}{3.3A_g} \right) \sqrt{f'_c} bd \quad (4)$$

$V_s$  is contributed by stirrups located within 45° diagonal shear cracks. Since all the stirrups are arranged in radial direction, they are not parallel with each other. So the gross angle of beam,  $\alpha$ , to be cut by 45° diagonal crack, may be calculated from geometry relationship[2] :

$$\alpha = \sin^{-1} \left( \frac{R}{r_i} \cos \vartheta \right) - \sin^{-1} \left( \frac{R}{r_o} \cos \vartheta \right) \quad (5)$$

where  $\vartheta$  is the angle between diagonal crack and centroid axis. If  $\theta_s$  is angle of stirrups,  $A_v$  is cross-sectional area of stirrups,  $f_y$  is yield stress of stirrup, we get

$$V_s = \frac{\alpha}{\theta_s} A_v f_y \quad (6)$$

Dowel force of tensile rebars is proposed by statistic :

$$V_d = 0.03 \cdot \sqrt[3]{A_s f_y} \quad (7)$$

Since rebars are not perpendicular to the critical section of diagonal shear cracks, the component of tensile force,  $T\alpha/2$ , would have positive contribution if the inner rebars are tension.  $T\alpha/2$  becomes negative if the outer rebars are tension. Consequently, ultimate shear capacity of RC curve beam is :

$$V_u = V_c + \frac{\alpha}{\theta_s} A_v f_y + V_d \pm \frac{1}{2} T\alpha \quad (8)$$

Comparing analytical results with test results, the error for loads of diagonal shear crack is from -16% to +16% and the error for loads of ultimate shear capacity is from -9% to +7%.

## EFFECTIVE CROSS-SECTIONAL AREA OF CURVE BEAMS

For a curve beam with depth to radius of centroid axis larger than 0.3, it is considered as thick arch. Strain energy of bending, shear and axial force should be taken into account for calculation of deflection by Castigliano Theorem. That is :

$$\Delta = \frac{\partial U}{\partial P} = \int_0^S \left\{ \frac{Mm}{AReE} + \frac{1.2Vv}{AG} + \frac{Nn}{AE} - \frac{Mn + nM}{ARE} \right\} dS \quad (9)$$

In which  $m = \partial M / \partial P$ ,  $v = \partial V / \partial P$ ,  $n = \partial N / \partial P$ ,  $A$  is effective cross-sectional area of curve beam,  $E$  is modulus of elasticity as code value,  $R$  is radius of centroid axis,  $e$  is eccentricity between centroid axis and neutral axis. Before flexural cracking,  $A$  is taken as  $A_g$ , gross cross-sectional area of curve beam. After flexural cracking,  $A$  is taken as  $A_{eff}$  :

$$A_{eff} = \left\{ \left( \frac{M_{cr}}{M_{max}} \right)^3 + \left[ I - \left( \frac{M_{cr}}{M_{max}} \right)^3 \right] \frac{I_{cr}}{I_g} \right\} A_g \quad (10)$$

In Eq.(10), the reduction ratio of ( $A_{eff} / A_g$ ) is equal to the flexural rigidity reduction ratio of ( $I_{eff} / I_g$ ) in ACI code. Eq.(10) valids until shear force at any section reaches  $V_y$  or reaches ultimate state of that section.  $V_y$  is the shear when softening of stiffness begins.  $V_y$  is proposed as :

$$V_y = V_c + 0.5V_s \pm 0.5T\alpha \quad (11)$$

Between  $V_y$  and ultimate load, the tangential  $A_{eff}$  is equal to  $1/3$  of the secant  $A_{eff}$  at  $V_y$  point calculated by Eq.(10). After ultimate point, the tangential  $A_{eff}$  is  $-1/3$  of the secant  $A_{eff}$  at  $V_y$  point for shear failure and  $-1/10$  of the secant  $A_{eff}$  at  $V_y$  point for flexural failure. Comparison of analytical and experimental results for vertical deflection at arch crown and for horizontal deflection at roller support are shown in Fig.6. Chen[2] and Lee[3] had more details about the comparison of  $P - \Delta$  curves.

## EQUIVALENT RECTANGULAR STRESS BLOCK FOR ULTIMATE BENDING MOMENT OF CURVE BEAMS

In order to simplify the calculation of the ultimate flexural capacity of RC curve beam, it would be nice to find out the magnitude and location of the concrete compression resultant under ultimate bending moment. Because the stress strain relationship of compressive concrete is nonlinear at ultimate state. The strain distribution in the cross-section of curve beam is nonlinear too. So the integrate of compression stress over the cross-section is rather complicate. This paper tries to propose the simplified contour maps for the magnitude and location of the concrete compression resultant  $C_c$ .

Consider a curve beam with compression stress distributed in  $kd$  depth as shown in Fig.7(a). Fig.7(b) is the equivalent stress block with equivalent stress  $\alpha \cdot f'_c$  and equivalent depth  $\beta_1 kd$ .  $\alpha$  and  $\beta_1$  may be calculated theoretically by :

$$\alpha\beta_1 = k_1 k_3 = \frac{C_c}{f'_c kd \cdot b} = \frac{I}{f'_c kd} \cdot \int_0^{kd} \sigma_{\theta,c} dy \quad (12)$$

$$\frac{\beta_1}{2} = k_2 = I - \frac{I}{kd} \cdot \frac{M_c}{C_c} = I - \frac{I}{kd} \cdot \frac{\int_0^{kd} \sigma_{\theta,c}(y) \cdot y dy}{\int_0^{kd} \sigma_{\theta,c}(y) dy} \quad (13)$$

For easy integrate of Eq.(12) and Eq.(13), let the stress-strain curve of compression concrete be the well-known Modified Hognestad's Equation [4], which is consisted of two parts :

1. Parabolic ascending part,  $0 \leq \varepsilon \leq \varepsilon_0$  :

$$\sigma_c(\varepsilon) = f_c'' \cdot \left[ 2 \cdot \left( \frac{\varepsilon}{\varepsilon_0} \right) - \left( \frac{\varepsilon}{\varepsilon_0} \right)^2 \right] \quad (14)$$

2. Linear descending part,  $\varepsilon_0 < \varepsilon \leq \varepsilon_u$

$$\sigma_c(\varepsilon) = f_c'' \cdot \left[ 1 - \gamma \cdot \left( \frac{\varepsilon - \varepsilon_0}{\varepsilon_u - \varepsilon_0} \right) \right] \quad (15)$$

in which,  $\varepsilon_0 = 1.8f_c''/E_c$  is the strain at maximum stress,  $E_c = 4700\sqrt{f_c''}MPa$  is the code specified slope in ascending part, the ultimate strain  $\varepsilon_u = 0.0038$ , the decreasing factor of stress from  $\varepsilon_0$  to  $\varepsilon_u$  in descending part  $\gamma = 0.15$ . Breen[5] and Attard[6] suggested that the maximum compression stress in flexure may be taken as the cylinder strength, that is  $f_c'' = f_c'$ , which gives a reasonably good agreement between the theoretical and experimental values.

If a curve beam is under positive bending moment, refer to  $y_1$  coordinate as shown in Fig.5, the tangential flexural strain at ultimate state may be calculated by :

$$\varepsilon_{\theta,p} = \varepsilon_{cu} \cdot \frac{r_o}{kd} \cdot \frac{y_1}{r_{na} + y_1} \quad (16)$$

in which  $\varepsilon_{cu} = 0.003$  is taken as that given in code. Introducing Eq.(15) and Eq.(16) into Eq.(12) and Eq.(13) for a curve beam with positive moment, we get :

$$(\alpha\beta_1)_p = (k_1k_3)_p = \left( \frac{\lambda_p - \omega}{\omega} \right) \cdot \xi_p \quad (17)$$

$$\left( \frac{\beta_1}{2} \right)_p = (k_2)_p = 1 - \left( \frac{\lambda_p - \omega}{\omega} \right) \cdot \frac{\xi_p}{\xi_p} \quad (18)$$

where

$$\lambda_p = \omega \cdot \frac{r_o}{kd} \quad (19)$$

$$\omega = \frac{\varepsilon_{cu}}{\varepsilon_0} \quad (20)$$

$$z = \frac{\gamma}{\varepsilon_u - \varepsilon_0} \quad (21)$$

$$\xi_p = 1 - 2\lambda_p + \frac{\omega}{\lambda_p - \omega} + \lambda_p z \varepsilon_0 \left( \frac{1 - \omega}{\lambda_p - \omega} \right) + 2\lambda_p (\lambda_p - 1) \cdot \ln \left( \frac{\lambda_p}{\lambda_p - 1} \right) + \lambda_p z \varepsilon_0 \cdot \ln \left( \frac{\lambda_p - 1}{\lambda_p - \omega} \right) \quad (22)$$

$$\begin{aligned} \zeta_p = & -\frac{1}{2} + 3\lambda_p + \frac{1}{2} \left( \frac{\omega}{\lambda_p - \omega} \right)^2 \left[ 1 - z\varepsilon_0 (\lambda_p - 1) \right] + \frac{z\varepsilon_0}{\lambda_p - 1} \left( \frac{1}{2} - \lambda_p \right) + \lambda_p z \varepsilon_0 \left( \frac{\omega}{\lambda_p - \omega} \right) \\ & + \lambda_p (3\lambda_p - 2) \cdot \ln \left( \frac{\lambda_p}{\lambda_p - 1} \right) - \lambda_p z \varepsilon_0 \cdot \ln \left( \frac{\lambda_p - 1}{\lambda_p - \omega} \right) \end{aligned} \quad (23)$$

Referring to  $y_2$  coordinate in Fig.5, if a curve beam is subjected to negative bending moment, the tangential flexural strain may be calculated by another equation :

$$\varepsilon_{\theta,n} = \varepsilon_{cu} \cdot \frac{r_i}{kd} \cdot \frac{y_2}{r_{na} - y_2} \quad (24)$$

Similarly, Eq.(12) and Eq.(13) for a curve beam with negative bending moment can be written as :

$$(\alpha\beta_1)_n = (k_1 k_3)_n = \left( \frac{\lambda_n + \omega}{\omega} \right) \cdot \xi_n \quad (25)$$

$$\left( \frac{\beta_1}{2} \right)_n = (k_2)_n = 1 - \left( \frac{\lambda_n + \omega}{\omega} \right) \cdot \frac{\zeta_n}{\xi_n} \quad (26)$$

where

$$\lambda_n = \omega \cdot \frac{r_i}{r_{na}} \quad (27)$$

$$\xi_n = -1 - 2\lambda_n + \frac{\omega}{\lambda_n + \omega} - \lambda_n z \varepsilon_0 \left( \frac{1 - \omega}{\lambda_n + \omega} \right) - 2\lambda_n (\lambda_n + 1) \cdot \ln \left( \frac{\lambda_n}{\lambda_n + 1} \right) + \lambda_n z \varepsilon_0 \cdot \ln \left( \frac{\lambda_n + 1}{\lambda_n + \omega} \right) \quad (28)$$

$$\begin{aligned} \zeta_n = & -\frac{1}{2} - 3\lambda_n + \frac{1}{2} \left( \frac{\omega}{\lambda_n + \omega} \right)^2 \left[ 1 + z \varepsilon_0 (\lambda_n + 1) \right] - \frac{z \varepsilon_0}{\lambda_n + 1} \left( \frac{1}{2} + \lambda_n \right) + \lambda_n z \varepsilon_0 \left( \frac{\omega}{\lambda_n + \omega} \right) \\ & - \lambda_n (3\lambda_n + 2) \cdot \ln \left( \frac{\lambda_n}{\lambda_n + 1} \right) + \lambda_n z \varepsilon_0 \cdot \ln \left( \frac{\lambda_n + 1}{\lambda_n + \omega} \right) \end{aligned} \quad (29)$$

Fig.8 shows the contour map of  $\beta_1/2$  for positive bending. Fig.9 shows the contour map of  $\alpha\beta_1$  for positive bending. Fig.10 and Fig.11 are the countour maps for negative  $\beta_1/2$  and  $\alpha\beta_1$  correspondingly. The resultant of equivalent stress block of curve beams may be find out easily from these countour maps.

## CONCLUSIONS

- 1.Flexural cracking moment and ultimate moment may be calculated by force equilibrium process, if the hypobolic strain distribution is considered for the cross-section of curve beam.
- 2.Cracking shear strength may be calculated by Eq.(3) or Eq.(4) which are similar to ACI code equation for straight beams. Ultimate shear capacity may be calculated by Eq.(8).
- 3.For thick arch, the effective cross-sectional area calculated by Eq.(10) would give the reasonable prediction of  $P - \Delta$  curve under monotonic loading.
4.  $\alpha$  and  $\beta_1/2$  calculated by Eq.(17), Eq.(18), and Eq.(25), Eq.(26) provide a good prediction for rectangular stress block for curve beam.
- 5.At ultimate flexural state, the resultant of equivalent concrete compression stress block may be find out easily from the contour maps shown in Fig.8 to Fig.11.

## REFERENCES

- 1.Tsai, Wan-Tsuang and Sheu Maw-Shyong (1995), " Design of RC Curve beams under Pure Bending", *Journal of the Chinese Institute of Civil and Hydraulic Engineering*, Taipei, Taiwan, Vol. 7, No. 4, June, pp545-548.
- 2.Chen, Chi-Huang (1998), " Test and Analysis of RC Curve Beams for Shear Behaviours", Master Thesis, *Dept. of Architecture, National Cheng-Kung Univ.*, Tainan, Taiwan.
- 3.Lee, Hou-Wei (1997), "Test and Analysis of RC Curve Beams for Flexural Behaviours", *Master Thesis, Dept. of Architecture, National Cheng-Kung Univ.*, Tainan, Taiwan.
- 4.E. Hognestad(1957), "Confirmation of Inelastic Stress Distribution in Concrete", *Journal of the Structural Division of the ASCE*, Vol. 83, No. ST2, pp.1189-1 – 1189-17.
- 5.Breen, J. E. 1962 , "The Restrained Long Concrete Column as a Part of a Rectangular Frame", Ph.D. dissertation, *Univ. of Texas at Austin*.
- M. M. Attard, M. M. Stewart 1998 , "A Two Parameter Stress Block for High-Strength Concrete," *ACI Structural Journal*, Vol. 95, No. 3, pp.305 - 317.

## ACKNOWLEDGEMENT

**Table 1 : Specimen Parameters**

Specimen No.	Tangential Reinforcement		Stirrup	$f'_c$ (MPa)	Ultimate Load (KN)	Failure Mode
	Exterior	Interior				
CB31	2-D13	3-D13	D10@ 6°	24.3	+225.0	Flexure
CB32	2-D13	3-D19	D13@ 6°	18.6	+490.5	Flexure
CB33	2-D13	3-D25	D13@ 6°	24.1	+630.2	Flexure
CB37	3-D13	3-D25	D13@ 6°	25.3	+420.0	Shear
CB38	3-D19	3-D25	D13@ 6°	25.2	+750.3	Flexure
CB41	3-D13	2-D13	D13@ 6°	18.6	+158.0	Flexure
CB42	3-D25	2-D13	D13@ 6°	20.6	+180.0	Flexure
CB51	3-D25	3-D25	D10@ 4°	22.2	+727.2	Shear
CB52	3-D19	3-D19	D10@ 6°	31.2	+467.5	Flexure
CB53	3-D19	3-D19	D10@ 4°, 8°	32.5	+473.3	Shear
CB54	3-D25	3-D25	D10@ 4°	22.2	-886.0	Shear
CB56	3-D19	3-D19	D10@ 4°, 8°	32.5	-609.9	Shear
CB60	3-D19	3-D19	D10@ 3°, 6°	24.1	+380.2	Shear
CB62	3-D19	3-D19	D10@ 6°	34.4	+398.8	Flexure
CB65	3-D25	3-D25	D10@ 6°	24.1	+525.0	Shear

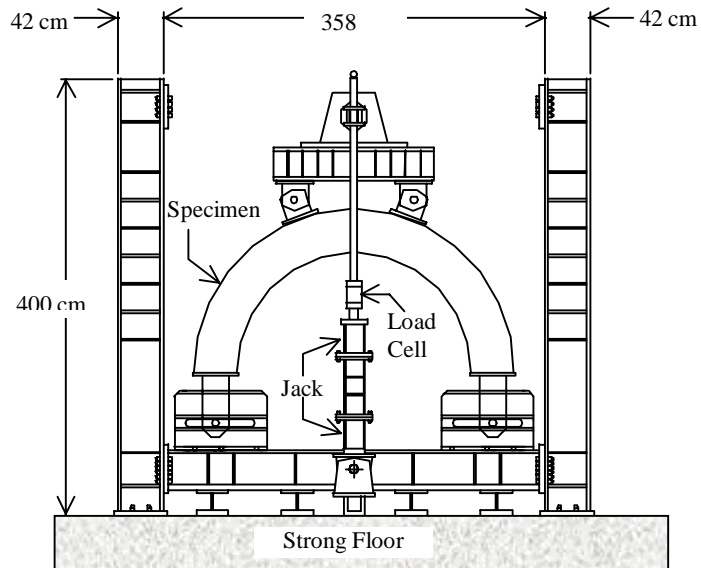


**Fig.1 Experimental Set Up**

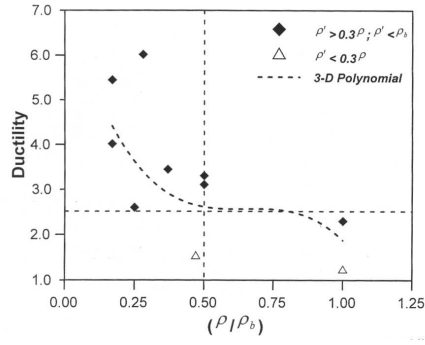


**Fig.2 Change of Curve Beam Ductility**

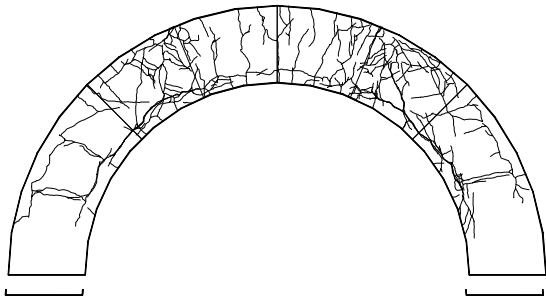


**Fig.3 Final Cracks for Flexural Failure**

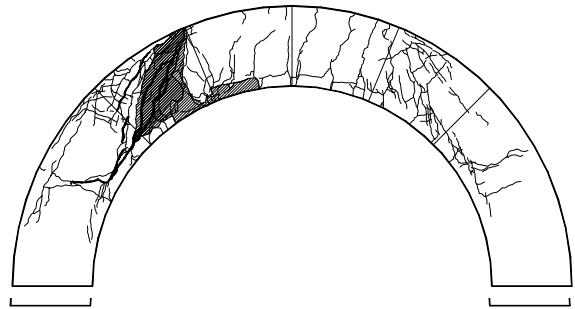


**Fig.4 Final Cracks for Shear Failure**

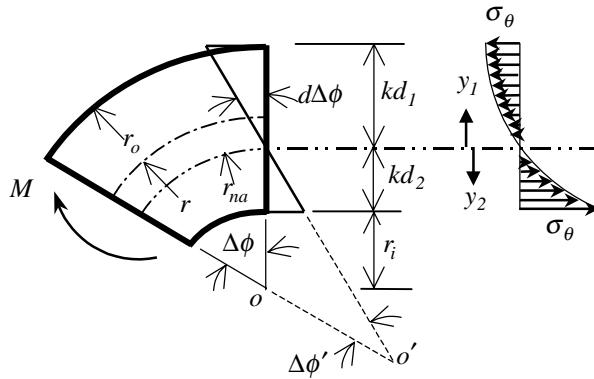


**Fig.5 Tangential Stress of Curve Beam**

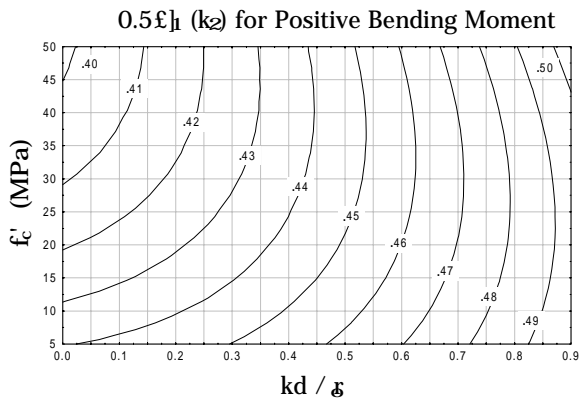


**Fig.6 Comparison of  $P - \Delta$  Curves for CB65**

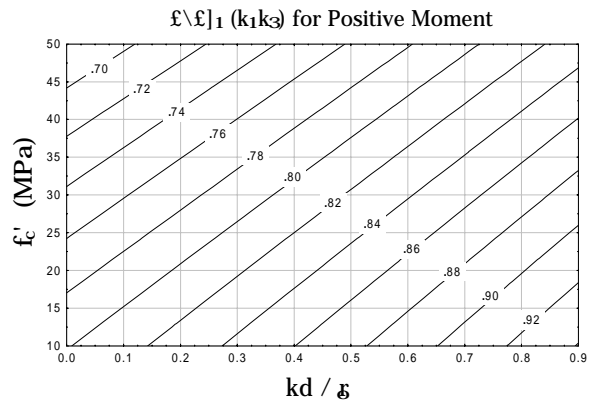


**Fig.7 Equivalent Stress Block of Curve Beam**

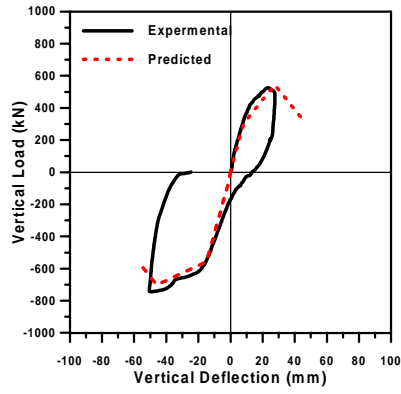


**Fig.8** Countour of  $0.5\beta_I$  Under Positive Bending Moment

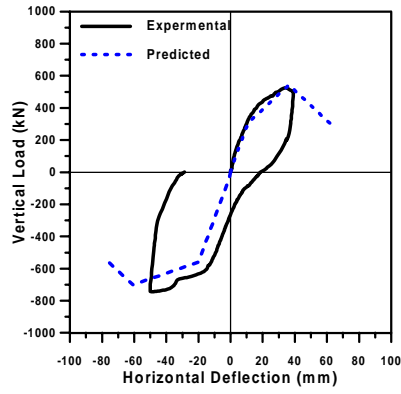


**Fig.9** Countour of  $\alpha\beta_I$  Under Positive Bending Moment

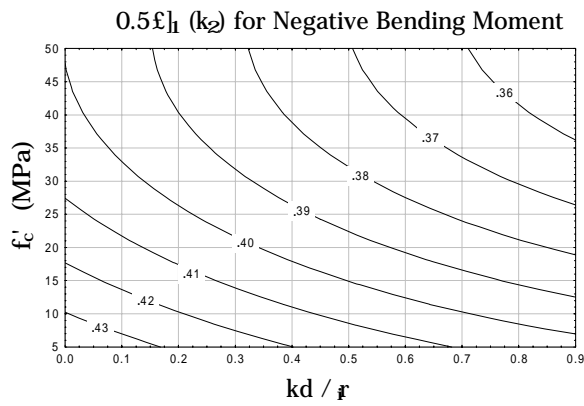


**Fig.10** Countour of  $0.5\beta_I$  Under Negative Bending Moment

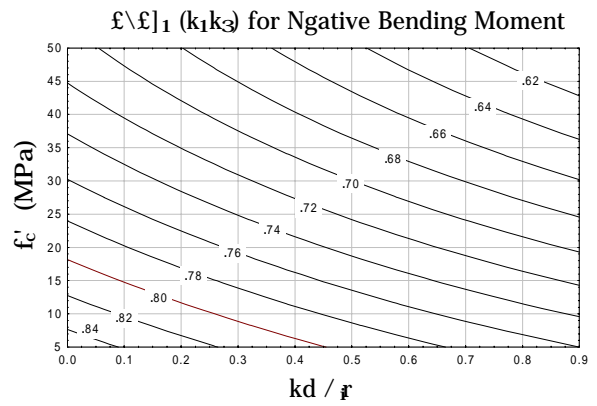


**Fig.11** Countour of  $\alpha\beta_I$  Under Negative Bending Moment